Ascorbate Inhibits the Carbethoxylation of Two Histidyl and One Tyrosyl Residues Indispensable for the Transmembrane Electron Transfer Reaction of Cytochrome b_{561}[†]

Fusako Takeuchi,[‡] Kazuo Kobayashi,[§] Seiichi Tagawa,[§] and Motonari Tsubaki*[,‡,||]

Department of Life Science, Faculty of Science, Himeji Institute of Technology, Kamigoori-cho, Akou-gun, Hyogo 678-1297, Japan, Institute for Protein Research, Osaka University, Suita, Osaka 565-0871, Japan, and Institute of Scientific and Industrial Research, Osaka University, Mihogaoka 8-1, Ibaraki, Osaka 567-0047, Japan

Received September 25, 2000; Revised Manuscript Received January 2, 2001

ABSTRACT: Cytochrome b_{561} from bovine adrenal chromaffin vesicles contains two heme B prosthetic groups and transports electron equivalents across the vesicle membranes to convert intravesicular monodehydroascorbate radical to ascorbate. We found previously that treatment of oxidized cytochrome b_{561} with diethyl pyrocarbonate caused specific *N*-carbethoxylation of three fully conserved residues (His88, His161, and Lys85) located at the extravesicular side. The modification lead to a selective loss of the electron-accepting ability from ascorbate without affecting the electron donation to monodehydroascorbate radical [Tsubaki, M., Kobayashi, K., Ichise, T., Takeuchi, F., and Tagawa, S. (2000) *Biochemistry 39*, 3276−3284]. In the present study, we found that these modifications lead to a drastic decrease of the midpoint potential of heme *b* at the extravesicular side from +60 to −30 mV. We found further that the *O*-carbethoxylation of one tyrosyl residue (Tyr218) located at the extravesicular side was significantly enhanced under alkaline conditions, leading to a very slow reduction process of the oxidized heme *b* with ascorbate. On the other hand, the presence of ascorbate during the treatment with diethyl pyrocarbonate was found to suppress the carbethoxylation of His88, His161, and Tyr218, whereas the modification level of Lys85 was not affected. Concomitantly, the final reduction level of heme *b* with ascorbate was protected, although the fast reduction phase was not fully restored. These results suggest that the two heme-coordinating histidyl residues (His88 and His161) are also a part of the ascorbate binding site. Tyr218 and Lys85 may have a role in the recognition/binding process for ascorbate and are indispensable for the fast electron transfer reaction.

In neurosecretory vesicles, such as adrenomedullary chromaffin vesicles and pituitary neuropeptide secretory vesicles, intravesicular ascorbate (AsA^-)[1] functions as the electron donor for copper-containing monooxygenases such as dopamine β-monooxygenase and peptidyl-glycine α-amidating monooxygenase (*1, 2*). Upon these monooxygenase reactions, monodehydroascorbate (MDA) radical is produced by univalent oxidation of AsA^- (*3*). Since neither AsA^- nor MDA radical can pass through the vesicle membranes (*4*−*6*), it is believed that the intravesicular MDA radical is reduced back to AsA^- by membrane-spanning cytochrome b_{561} and subsequently the oxidized cytochrome b_{561} is reduced by AsA^- in the extravesicular side (i.e., the cytosolic side). Thus, cytochrome b_{561} acts as a transmembrane electron carrier which catalyzes a long-range electron transfer between two cellular compartments. It is reported that this cytochrome has a favorable midpoint oxidation−reduction potential of +140 mV (*7*). Indeed, among various cytochromes, cytochrome b_{561} is unique in its localization to neuroendocrine cells in adrenal medulla, gut, pituitary, and different regions of brain (*8, 9*).

Cytochrome b_{561} is a highly hydrophobic hemoprotein (*10, 11*) with a molecular mass of 29 kDa (*11*). The purified cytochrome b_{561} contains two distinct heme *b* centers (*12*). In the oxidized state, one heme *b* showed the usual low-spin EPR signal ($g_z = 3.14$), and the other gave a highly anisotropic low-spin EPR signal ($g_z = 3.70$) (*12*). Our pulse radiolysis study showed that the two heme *b* centers have a distinct role for electron donation to MDA radical and electron acceptance from AsA^-, respectively (*13*). On the basis of comparison of the deduced amino acid sequences of seven species, we have proposed a plausible structural model of cytochrome b_{561} (*14*). In the proposed model (Figure 1), there are two fully conserved regions in the sequences; the first one (^{69}ALLVYRVFR^{77}) is located on

[†] This work was supported by Grants-in-Aid for Scientific Research on Priority Areas (A) (10129226 to M.T.; 08249104 to K.K.; 12050236 to M.T.) and (B) (12147205 to K.K.) and Scientific Research (C) (10680638 to M.T.) from the Japanese Ministry of Education, Science, Sports and Culture and by a grant from the Hyogo Science and Technology Association (1998, to M.T.).

* Address correspondence to this author at the Department of Life Science, Faculty of Science, Himeji Institute of Technology, Kohto 3-2-1, Kamigoori-cho, Akou-gun, Hyogo 678-1297, Japan. Fax: +81-791-58-0189. Tel: +81-791-58-0189. E-mail: tsubaki@sci.himeji-tech.ac.jp.

[‡] Department of Life Science, Himeji Institute of Technology.

[§] Institute of Scientific and Industrial Research, Osaka University.

[||] Institute for Protein Research, Osaka University.

[1] Abbreviations: AsA^-, ascorbate monoanion form; AsA^{2-}, ascorbate dianion form; MDA, monodehydroascorbate; DEPC, diethyl pyrocarbonate; MALDI-TOF, matrix-assisted laser desorption/ionization-time-of-flight.

10.1021/bi002240x CCC: $20.00
Published on Web 03/03/2001

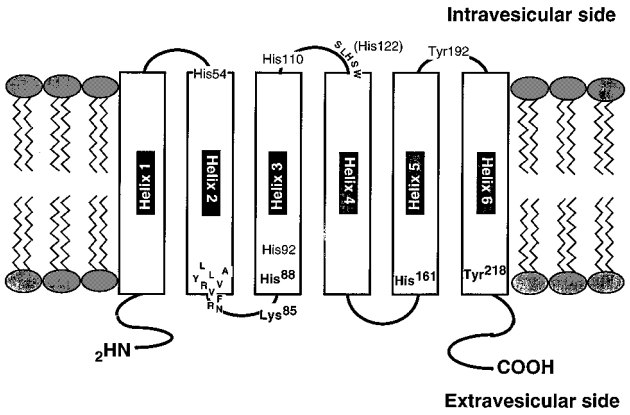

FIGURE 1: Transmembrane structural model of cytochrome b_{561}. The two fully conserved sequences, six histidyl residues (which include two major DEPC modification sites; His88 and His161), and one lysyl residue (Lys85) are indicated, in addition to two other DEPC modification sites (Tyr218 and Tyr192) (*15*).

the extravesicular side of the α-helical segment, and the second one (^{120}SLHSW^{124}) is located in an intravesicular loop connecting two α-helical segments, respectively (*14*). These conserved sequences may form a part of the binding sites for extravesicular AsA^- and intravesicular MDA radical, respectively (*14*). The two hemes *b* may be located on each side of the vesicular membranes in close contact with these binding sites, respectively (*14*).

In a previous report, we found that the fast electron-accepting ability of cytochrome b_{561} from AsA^- was selectively destroyed by treatment with diethyl pyrocarbonate (DEPC) in the oxidized state (*15*). However, the electron-donating activity from reduced heme *b* center to MDA radical was retained after the DEPC treatment. Three major DEPC modification sites (His88, His161, and Lys85) and three minor modification sites, including Tyr218, were identified by matrix-assisted laser desorption/ionization-time-of-flight (MALDI-TOF) mass spectrometric analyses (Figure 1) (*15*). In the present study, we further analyzed the reaction of DEPC with purified cytochrome b_{561} in the presence of ascorbate. We report here that both the carbethoxylation of His88, His161, and Tyr218 residues and the electron-accepting ability were protected by the presence of ascorbate during the DEPC treatment.

MATERIALS AND METHODS

Purification of Cytochrome b_{561}. Cytochrome b_{561} was purified to a homogeneous state, as described previously (*12*). The purity of cytochrome b_{561} was analyzed with visible absorption spectra, heme content analysis, and SDS−polyacrylamide gel electrophoresis (*12*). Before use, purified cytochrome b_{561} was concentrated to around 100 μM in an Amicon concentrator using a membrane filter (MWCO = 30 000; Millipore). All other reagents were commercially obtained as analytical grade. The concentration of cytochrome b_{561} was determined using a millimolar extinction coefficient of 267.9 mM^{-1} cm^{-1} at 427 nm in the reduced state (*12*).

Modification of Cytochrome b_{561} with Diethyl Pyrocarbonate. Concentrated cytochrome b_{561} solution was acidified to pH 6.5 by adding 0.5 M potassium phosphate buffer (pH 6.0) and was oxidized by stepwise additions of 100 mM potassium ferricyanide solution. Complete oxidation was checked with visible absorption spectroscopy. The oxidized cytochrome b_{561} was gel-filtered through a Sephadex G-25f column equilibrated with 50 mM potassium phosphate buffer (pH 6.5) containing 1.0% (w/v) octyl β-glucoside and was, then, diluted with the same buffer to an appropriate concentration. The diluted sample was treated with various concentrations of DEPC for 30 min, as previously described (*15*). The DEPC treatment of cytochrome b_{561} in the reduced state was done similarly, except for the presence of either 2.0 or 20 mM sodium ascorbate or 5 mM sodium dithionite. The pH dependency of the DEPC modification was done similarly, except for the buffer systems: 50 mM sodium acetate buffer for pH 4.9 and 5.4, 50 mM potassium phosphate buffer for pH 6.0 and 7.1, 50 mM sodium-HEPES or Tris-HCl buffer for pH 8.1, and 50 mM sodium-Tricine buffer for pH 9.2.

The DEPC-treated samples were gel-filtered through a Sephadex G-25f column equilibrated with 50 mM potassium phosphate buffer (pH 6.5) containing 1.0% (w/v) octyl β-glucoside to remove unreacted DEPC. The DEPC-treated cytochromes b_{561} were then analyzed for the reactivity with AsA^- with a Shimadzu UV-2400PC spectrophotometer. Finally, the sample was fully reduced with sodium dithionite, and its absorption spectrum was recorded to check the integrity of the heme moiety. The reduction level was analyzed with the absorbance at both 561 nm (α-band) and 427 nm (Soret band) by normalizing against the level of the dithionite-reduced state.

Redox Titration. Spectrophotometric titrations were performed essentially as described by Dutton (*16*), using a Shimadzu UV-2400PC spectrometer equipped with a thermostated cell holder connected to a thermobath (RC6 CS, LAUDA) and a custom anaerobic cuvette (1 cm light path, 5 mL sample volume) equipped with a combined platinum and Ag/AgCl electrode (6860-10C, Horiba, Tokyo, Japan), and a screw-capped sidearm was used. Oxidized cytochrome b_{561} sample in 50 mM potassium phosphate buffer (pH 6.0) containing 1.0% (w/v) octyl β-glucoside was mixed with redox mediators (potassium ferricyanide, 60 μM; quinhydrone, 20 μM; 1,2-naphthoquinone, 20 μM; phenazine methosulfate, 20 μM; duroquinone, 40 μM; 2-hydroxy-1,4-naphthoquinone, 5 μM; riboflavin, 20 μM). After being passed through a cellulose acetate filter (DISMIC-25cs, 0.45 μm; Toyo Roshi Kaisha, Ltd., Tokyo, Japan), the sample solution was placed in the cuvette. The sample was kept under a flow of moistened argon gas (Koatsugasu Kogyo, Takasago, Japan) to exclude oxygen and was continuously stirred with a small magnetic stirrer (CC-301, SCINICS, Tokyo, Japan). Reductive titration was performed at 20 °C by addition of small aliquots of sodium dithionite (5 mM) solution through a needle in the rubber septum on the sidearm; for subsequent oxidative titration, potassium ferricyanide (5 mM) was used as the titrant. The changes in absorbance ($A_{560.0}$ minus $A_{566.8}$, the isosbestic point of cytochrome b_{561}) were corrected with the dilution effect and analyzed with KaleidaGraph (v. 3.05) employing a Nernst equation with a single or two redox components.

Pulse Radiolysis. Pulse radiolysis experiments were performed with an electron linear accelerator at the Institute of Scientific and Industrial Research, Osaka University, as previously described (*13, 17, 18*). The pulse width and energy were 8 ns and 27 MeV, respectively. The sample was placed

in a quartz cell with an optical path length of 1.0 cm. The temperature of the sample was maintained at 20 °C. A 150 W halogen lamp was used as the light source. After passing through the optical path, the transmitted light intensities were analyzed and monitored by a fast spectrophotometric system composed of a Nikon monochromator, an R-928 photomultiplier, and a Unisoku data analyzing system. Under the conditions employed here, the primary radical products [hydrated electron (e_{aq}^-), OH•, and H•] were efficiently converted to MDA radical at a concentration range of 20−30 μM in the presence of N_2O-saturated 10 mM AsA^-.

Samples of cytochrome b_{561} for pulse radiolysis were prepared as follows. Oxidized cytochrome b_{561} (29 μM) in 10 mM potassium phosphate buffer (pH 7.0) containing 1.0% (w/v) octyl β-glucoside was treated with 0.5 mM DEPC for 1 h on ice. Similarly, reduced cytochrome b_{561} in the presence of AsA^- (or sodium dithionite) was treated with 0.5 mM DEPC. Then the sample was gel-filtered against 10 mM potassium phosphate buffer (pH 7.0) containing 1.0% (w/v) octyl β-glucoside and 10 mM AsA^-. Untreated or DEPC-treated cytochrome b_{561} was further diluted with the same buffer to make a final concentration of cytochrome b_{561} at 14.5 μM. The sample solutions were bubbled with N_2O gas for 5 min before pulse radiolysis. For each measurement, a fresh sample was used, even though pulse radiolysis did not cause any damage to the sample as judged by its visible absorption spectrum.

Protease Digestion of Cytochrome b_{561}. The digestion was started by addition of protease to oxidized cytochrome b_{561} solution (~50 μM) in 50 mM potassium phosphate (pH 6.5) buffer containing 1.0% octyl β-glucoside at room temperature. Final concentrations of the protease used were 0.76 μM for TPCK-treated trypsin (from bovine pancreas; Sigma Chemical Co., St. Louis, MO) and 1.48 μM for V8 protease (from *Staphylococcus aureus* V8; Wako Pure Chemical Industries, Ltd., Osaka, Japan), respectively. The extent of the digestion was checked with mass spectrometric analysis with an appropriate interval.

MALDI-TOF Mass Spectrometry. Mass spectrometric analyses were carried out on a Voyager RP mass spectrometer (Perseptive Biosystems, Farmingham, MA) using a 20 kV accelerating voltage. The mass spectra were acquired by adding the individual spectra from 256 laser shots. For protein analysis, the samples were run in a linear mode and for peptide analysis in a reflector mode. The protein solutions were diluted 1:9 (v/v) with a matrix solution, 3,5-dimethoxy-4-hydroxycinnamic acid (Aldrich, Gillingham, England), 50 mg/mL in 30% acetonitrile in 0.3% TFA. The peptide solutions were diluted 1:9 (v/v) with a matrix solution, α-cyano-4-hydroxycinnamic acid (Aldrich, Gillingham, England), 50 mg/mL in 50% acetonitrile in 0.3% TFA. The mixtures (typically 1.0 μL) were deposited on the sample plate and allowed to air-dry before analysis. Insulin (bovine, 5733.69 Da), thioredoxin (*Escherichia coli*, 11 673.68 Da), and apomyoglobin (horse, 16 951.56 Da) were used as external standards for the protein analysis. Angiotensin I (1296.51 Da), ACTH (clips 1−17, 2093.46 Da; clips 18−39, 2465.72 Da; clips 7−38, 3659.19 Da), and insulin (bovine, 5733.69 Da) were used as external standards for the peptide analysis. Insulin (bovine, 5733.69 Da) was also used as a control protein for the level of the DEPC modification in the presence or absence of AsA^-.

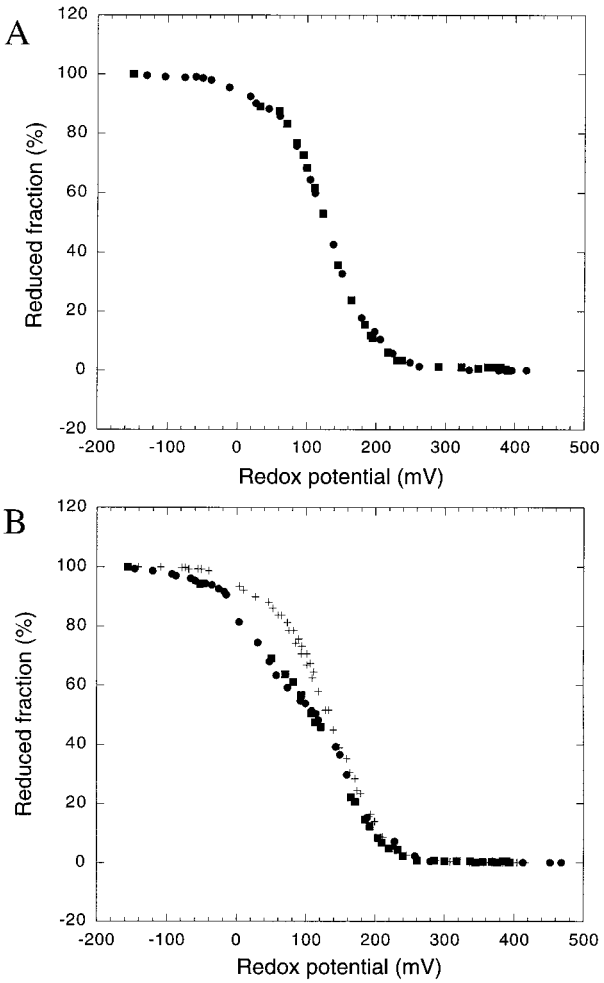

FIGURE 2: Potentiometric redox titrations of purified cytochrome b_{561} before (A) and after (B) DEPC (0.5 mM) treatment in the absence or presence of 20 mM AsA^-. The fraction of reduced cytochrome b_{561} was plotted against the solution potential. Potentials are expressed relative to the normal hydrogen electrode (NHE). Solid circles and squares indicate data points for the reductive and the oxidative titrations, respectively. In panel B, data points for the DEPC-treated cytochrome b_{561} in the presence of 20 mM AsA^- are indicated by crosses for both the reductive and the oxidative titrations. Other details are described in the text.

The positions of the protease cleavage sites in the cytochrome b_{561} amino acid sequence were identified by considering the molecular masses of the polypeptide fragments detected by MALDI-TOF mass spectrometry and the specificity of the proteases used. The search of the corresponding fragments in the amino acid sequence of cytochrome b_{561} was carried out using the program GPMAW (v 3.15) (Lighthouse Data, Odense M, Denmark). The molecular masses of all polypeptides measured matched the theoretical ones, obtained from the bovine cytochrome b_{561} amino acid sequence (*19*), within an accuracy of 0.1% or better.

RESULTS

The potentiometric behavior of purified cytochrome b_{561} is shown in Figure 2A. There is good agreement between points obtained during reductive and oxidative titrations. The apparent midpoint potential was estimated around +125 mV, being consistent with previous reports for purified cytochrome b_{561} (*20*) and for membrane preparations (*7*, *21*). The Nernst plot [i.e., redox potential vs log ([ox]/[red])] of the

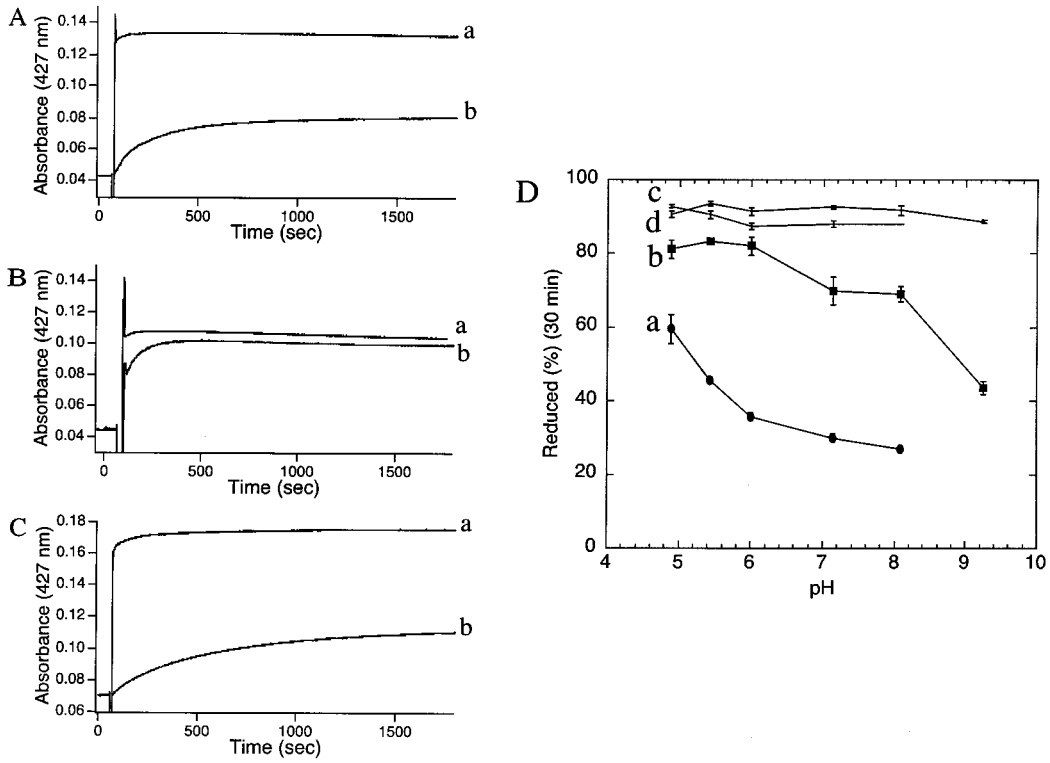

FIGURE 3: Time courses of the absorption change at 427 nm upon addition of 2 mM AsA^- to the oxidized DEPC (0.5 mM)-treated [at pH 6.5 either in the oxidized state (panel A) or in the presence of 20 mM AsA^- (panel B), and at pH 8.1 in the oxidized state (panel C)] cytochrome b_{561} and the pH dependency of the DEPC-dependent inactivation of the electron-accepting ability from AsA^- (panel D). Cytochrome b_{561} [11.2 μM in 1.0% octyl β-glucoside, 50 mM potassium phosphate buffer (pH 6.5) or in 1.0% octyl β-glucoside, 50 mM Tris-HCl buffer (pH 8.1)] was treated with 0.5 mM DEPC for 30 min, and was gel-filtrated. An optical quartz cell (light path, 1.0 cm) containing 1.0 mL of the control (trace **a**) or the DEPC (0.5 mM)-treated (trace **b**) oxidized cytochrome b_{561} was placed in the spectrophotometer. Twenty microliters of AsA^- solution (100 mM in the buffer) was added (final concentration, 2.0 mM), and the absorption change at 427 nm was recorded in the time-scan mode at room temperature for 30 min (panels A−C). The electron-accepting abilities from AsA^- of the samples treated with DEPC at various pHs either in the oxidized state (trace **a**) or in the presence of 20 mM AsA^- (trace **b**) were plotted against the pH in comparison with the corresponding controls (traces **c** and **d**, respectively) (panel D). The electron-accepting abilities from AsA^- were expressed as the percentage of the reduction level of heme *b* 30 min after the mixing. The vertical bar at each data point indicates the standard deviation (3 measurements). Concentrations of cytochrome b_{561} from the 'AsA^--mixing assay' were 0.52 μM (panels A, C, and D) and 0.42 μM (panel B).

data showed a sigmoid shape, and a slope with 79 mV, which is much greater than the 59 mV predicted by the Nernst equation with a single redox component (data not shown). The upper and lower asymptotic potentials in the plot were estimated as +170 and +60 mV, respectively, very similar to those reported previously (*20*). These results are fully consistent with the presence of two heme *b* centers with a different midpoint potential. Treatment with DEPC (0.5 mM) in the oxidized state caused a drastic change in the redox behavior of the heme *b* component having a lower potential, suggesting a significant downshift of its midpoint potential (Figure 2B). The Nernst plot showed that DEPC treatment caused a shift of the lower asymptotic potential to as low as −30 mV (data not shown). On the other hand, the higher asymptotic potential did not show any appreciable influence upon the treatment. The presence of 20 mM AsA^- during the DEPC treatment inhibited the anomalous redox behavior (Figure 2B) and the downshift of the lower asymptotic potential almost completely.

Electron-accepting ability from AsA^- was assayed for DEPC-treated cytochrome b_{561} (in the absence or presence of AsA^-). In a control assay, untreated cytochrome b_{561} was found to be reduced with 2 mM AsA^- very quickly to a reduction level of 85−90% (Figure 3A, trace **a**). In contrast, when the cytochrome b_{561} sample treated with 0.5 mM DEPC in the oxidized state (at pH 6.5) was mixed with 2 mM AsA^-, less than half of the heme moiety was reduced with a very slow reaction process (Figure 3A, trace **b**). The presence of 20 mM AsA^- during the treatment with DEPC restored the final reduction level with AsA^- close to that of the untreated sample (Figure 3B, traces **a** and **b**). However, the fast electron transfer phase from AsA^- to oxidized heme *b* observed for the untreated sample was not fully rescued (Figure 3B, trace **b**). It is important to note that the dithionite-reduced spectra of the control and the DEPC-treated (either with or without AsA^-) samples were indistinguishable from each other (spectra not shown). This observation suggests that the carbethoxylation did not cause any drastic structural damage around the heme *b* moiety.

The electron-accepting ability from AsA^- was assayed similarly for the samples treated with 0.5 mM DEPC at various pH conditions ranging from 4.9 to 9.2 (Figure 3D). The DEPC treatment in the oxidized state caused a significant inactivation of the activity as judged by the final reduction level with AsA^- (Figure 3D, trace **a**). Only for the samples treated at lower pH (4.9 and 5.4) was the inactivation somewhat relieved. It must be noted that the treatment of oxidized cytochrome b_{561} with DEPC under alkaline conditions caused a further retardation of the heme reduction process with AsA^- (Figure 3C), although the final reduction

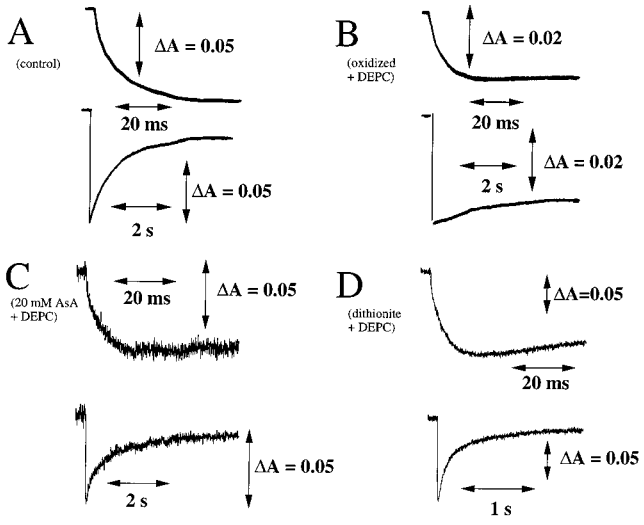

FIGURE 4: Reactions with MDA radical (upper traces) of the reduced heme *b* of control (A) and the DEPC (0.5 mM)-treated samples of cytochrome b_{561} in the oxidized state (B) or in the reduced states [in the presence of 20 mM ascorbate (C) and 5 mM sodium dithionite (D)] and the following reactions with AsA^- (lower traces) of the oxidized heme *b* of the corresponding samples after pulse radiolysis. The reaction mixture contained 5.2 μM cytochrome b_{561}, 5 mM AsA^-, 1.0% octyl β-glucoside, 10 mM potassium phosphate buffer (pH 7.0). The absorption changes were monitored at 430 nm for both the faster (upper traces) and the slower (lower traces) phases at room temperature.

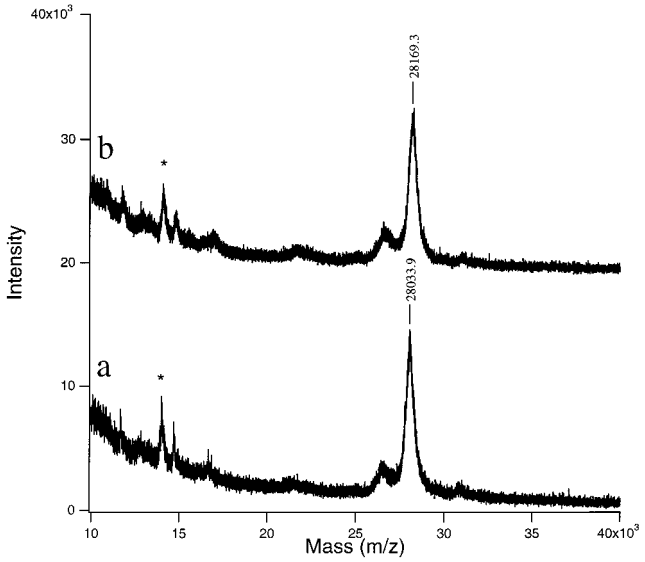

FIGURE 5: MALDI-TOF mass spectra of cytochrome b_{561} before (trace **a**) and after (trace **b**) DEPC (0.5 mM) treatment in the presence of 20 mM AsA^-. Mass spectra were obtained as described in the text. The peak around 26 500 (*m*/*z*) is probably due to a partially cleaved form of cytochrome b_{561}.

level was not much different from those treated with DEPC in a neutral or acidic condition (Figure 3A). In a neutral pH region, the presence of 20 mM AsA^- during the DEPC treatment caused a significant protective effect (Figure 3D, trace **b**). For the samples treated in an alkaline pH region, the protective effect of AsA^- was diminished.

The electron transfer activity to MDA radical was examined by the pulse radiolysis method for the DEPC-treated cytochrome b_{561}. MDA radical oxidized quickly the reduced heme *b* center of untreated cytochrome b_{561} (Figure 4A, upper trace) with a second-order rate constant of 1.2×10^6 M^{-1} s^{-1} at pH 7.0. Pretreatment with DEPC in various conditions (such as in the oxidized state, in the presence of 20 mM AsA, and in the presence of 5 mM sodium dithionite) did not cause any appreciable influence on the fast oxidation process of heme *b* (Figure 4B,C, upper traces). These observations indicate that the electron-donating ability of the reduced heme *b* to MDA radical was not influenced appreciably by the DEPC treatment. On the other hand, the following second phase due to the rereduction of the oxidized heme *b* with AsA^- was completely lost upon DEPC treatment in the oxidized state (Figure 4B, lower trace), but was fully protected in the presence of 20 mM AsA^- (Figure 4C, lower trace). The presence of sodium dithionite (5 mM) during the DEPC treatment also showed the protective effect against the loss of the rereduction of oxidized heme *b* with AsA^- (Figure 4D).

The mass spectrum of intact cytochrome b_{561} in the presence of 1.0% octyl β-glucoside was directly analyzed in a linear mode. The spectrum showed a clear $[M+H^+]$ peak at 28 030 (*m*/*z*) (Figure 5, trace **a**). This value is slightly higher than the theoretical value of 27 901.9 based on the deduced amino acid sequence (*19*). The DEPC (0.5 mM) treatment in the oxidized state caused a mass shift to 28 250 (*m*/*z*) (not shown), consistent with the introduction of about three carbethoxy groups (73.0 Da × 3) per one molecule of cytochrome b_{561}. The DEPC (0.5 mM) treatment of cytochrome b_{561} in the presence of 20 mM AsA^- made the mass shift smaller to 28 160 (*m*/*z*) (Figure 5, trace **b**). This result suggests that a part of the reactive sites (about 1.2 residues/molecule) was protected against the DEPC modification by the inclusion of AsA^-.

To identify the protected sites with AsA^-, we conducted MALDI-TOF mass spectrometric analyses of a tryptic digest from cytochrome b_{561}. The untreated cytochrome b_{561} showed many partially cleaved polypeptides (Figure 6, trace **a**). We had identified most of these polypeptides, as previously reported (*15*). Mass analyses of a tryptic digest from the DEPC-treated sample in the oxidized state showed several singly, doubly, and triply modified polypeptides as indicated by a mass shift by +72, +144, and +216 (*m*/*z*), respectively (Figure 6, trace **c**). In addition, there were many polypeptides exhibiting much larger shifts, which could not be explained by the usual *N*-carbethoxylation of histidyl residues. We found that these unusual peaks were caused by a selective *N*-carbethoxylation of one conservative lysyl residue (Lys85), resulting in a noncleavable site upon tryptic digestion. Thus, we concluded previously that there were three major DEPC modification sites at Lys85, His161, and His88 for oxidized cytochrome b_{561} (*15*).

A typical mass spectrum of a tryptic digest obtained from the sample pretreated with DEPC in the presence of 20 mM AsA^- is shown in Figure 6 (trace **b**). The spectrum indicates that the intensities of the peptides containing Val86 at the NH_2-terminus (such as peptides 86−111, 86−112, and 86−113) became very weak compared to those obtained from the control sample (Figure 6, trace **a**). A careful comparison with the spectrum of the DEPC-treated sample in the oxidized state (Figure 6, trace **c**) showed that the *N*-carbethoxylation of Lys85 occurred even more significantly in the presence of 20 mM AsA^- than in the oxidized state. This can be evidenced by the almost complete absence of

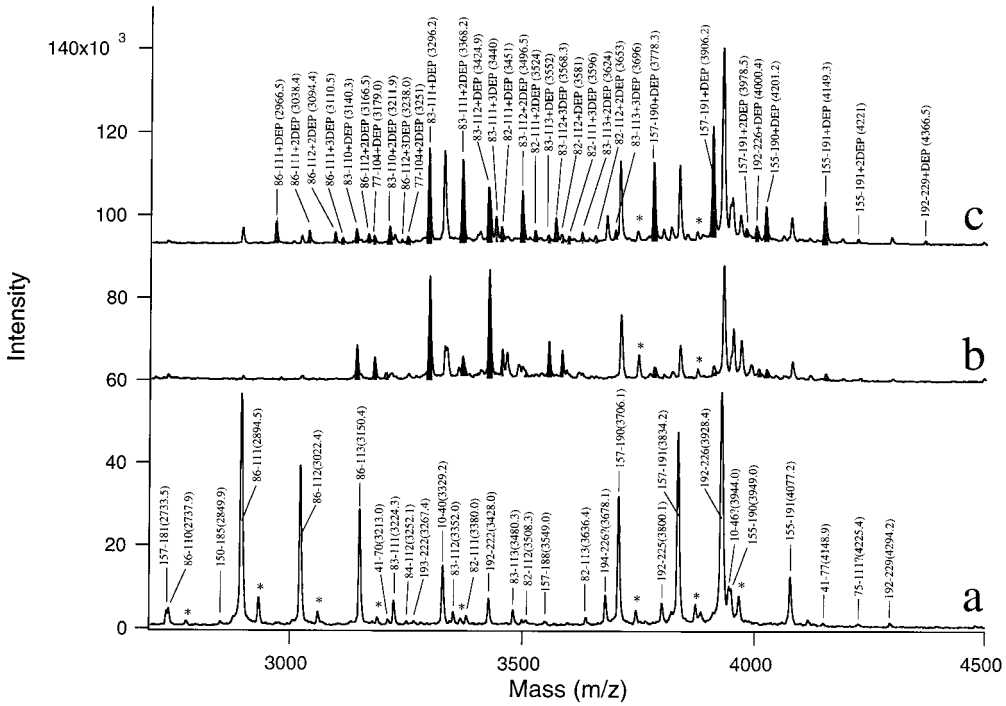

FIGURE 6: MALDI-TOF mass spectra of tryptic digests obtained from the untreated (trace **a**) and the DEPC (0.5 mM)-treated [either in the presence of 20 mM AsA^- (trace **b**) or in the oxidized state (trace **c**)] cytochrome b_{561}. Tryptic digests were obtained as described in the text. A mixture of the polypeptides was directly analyzed with MALDI-TOF mass spectrometry. Other conditions are described in the text. The number for each peak indicates the assignment of each polypeptide by a range of amino acid residues. The peaks corresponding to polypeptides containing a carbethoxy group are shaded, and the number of carbethoxy groups introduced into the polypeptide is indicated (e.g., "+2DEP"). The number in parentheses indicates the observed mass value (*m*/*z*) for each peak. Peaks indicated by an asterisk are due to $[M+K^+]$ species.

the peptides containing Val86 at the NH_2-terminus (such as peptides 86−111+DEP, 86−111+2DEP, 86−112+DEP, and 86−112+2DEP) in Figure 6 (trace **b**). On the other hand, the extent of modification at His88 and His161 was suppressed drastically when the DEPC treatment was performed in the presence of AsA^- (Figure 6, traces **b** and **c**). The suppression can be clearly seen in the spectra as the decrease in intensity of the DEPC-modified peptides, such as 157−190+DEP, 157−191+DEP, and 155−191+DEP for the modification at His161 and 83−111+2DEP and 83−112+2DEP for the modification at His88, respectively. The absence of any other unusual peaks in the mass spectra suggests that no new DEPC modification site(s) was (were) formed in cytochrome b_{561} upon inclusion of AsA^-. Similar results were obtained when the DEPC treatment was performed in the presence of 5 mM sodium dithionite (results not shown).

To clarify further the protective effect of AsA^- against DEPC modification, mass analyses of V8 peptides from the DEPC-treated cytochrome b_{561} were also performed (Figure 7). Three V8 peptides, 188−233, 188−232, and 199−232, produced corresponding +72 (*m*/*z*) peaks, respectively (Figure 7, traces **a** and **c**). But, the extents of modification were much reduced compared to those pretreated with DEPC in the oxidized state (Figure 7, trace **b**), indicating that *O*-carbethoxylation of Tyr218 was also suppressed significantly upon inclusion of AsA^- during the DEPC treatment. Similar results were obtained when the DEPC treatment was done in the presence of 5 mM sodium dithionite (results not shown).

Although the middle part of cytochrome b_{561} did not give V8 peptides in significant amounts in the mass spectra, there were several weak peaks derived from this part. One V8 peptide, 68−126, was shown to contain four DEPC modification sites (two major sites at Lys85 and His88, two minor sites at His92, and one unidentified site), giving a ∼60:40 mixture of 68−126+2DEP and 68−126+4DEP in the oxidized state (Figure 8A, traces **a** and **c**). The extent of the DEPC modification was significantly suppressed in the presence of AsA^- (Figure 8A, trace **b**); now 68−126+DEP and 68−126+2DEP were the major species. Another V8 peptide, 73−95, was also shown to contain three DEPC modification sites (two major sites at Lys85 and His88 and one minor site at His92) (Figure 8B, traces **a** and **c**). The sample treated in the oxidized state gave 73−95+2DEP as a major species (Figure 8B, trace **c**), whereas the sample treated in the presence of AsA^- produced two kinds of DEPC-modified peptides, one major species of 73−95+DEP and a minor one of 73−95+2DEP (Figure 8B, trace **b**). Since the extent of the DEPC modification at Lys85 was even stronger in the presence of AsA^-, the DEPC modification at His88 might be significantly suppressed upon inclusion of AsA^- (Figure 8B, trace **b**). This result is consistent with that obtained from the analyses for the tryptic digest.

The tryptic and V8 protease digests of the sample treated with DEPC in the alkaline condition (pH 8.1) were also examined by MALDI-TOF mass analyses. We found that the tryptic peptides in the higher mass region showed a significant enhancement of the modification with DEPC as indicated by a mass shift by +72 (*m*/*z*) (Figure 9). These polypeptides (such as 192−235, 192−236, and192−240) contain two possible modification sites, Tyr218 and Tyr192, as previously reported (*15*). However, the mass analyses of theV8 peptides from the sample treated with DEPC in an

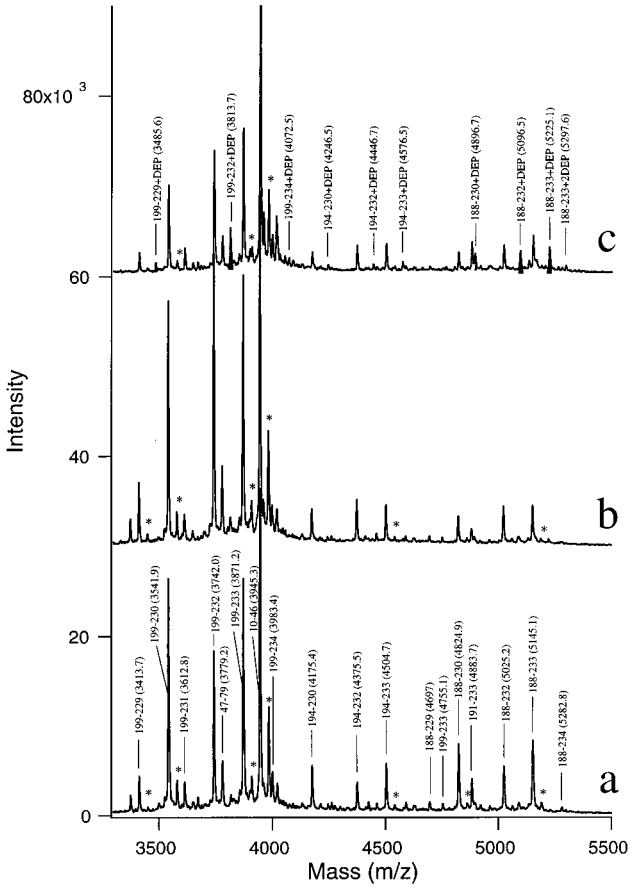

FIGURE 7: MALDI-TOF mass spectra of V8 protease digests obtained from the untreated (trace **a**) and the DEPC (0.5 mM)-treated [either in the presence of 20 mM AsA^- (trace **b**) or in the oxidized state (trace **c**)] cytochrome b_{561}. V8 protease digests were obtained as described in the text. A mixture of the polypeptides was directly analyzed with MALDI-TOF mass spectrometry. Other conditions are the same as in the legend to Figure 6.

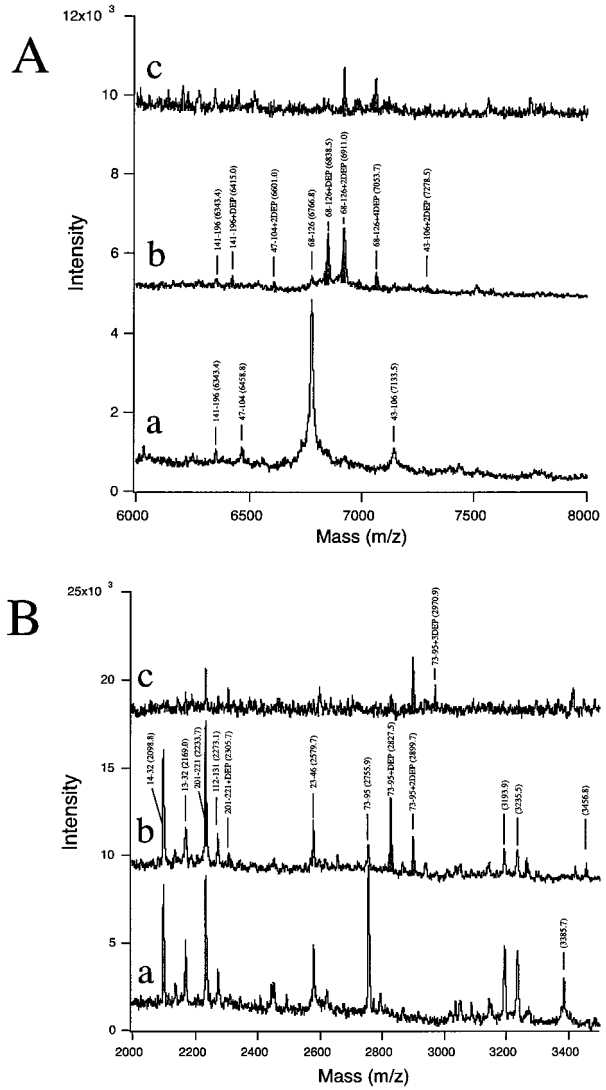

FIGURE 8: Parts of the MALDI-TOF mass spectra of V8 protease digests obtained from the untreated (trace **a**) and the DEPC (0.5 mM)-treated [either in the presence of 20 mM AsA^- (trace **b**) or in the oxidized state (trace **c**)] cytochrome b_{561}. V8 protease digests were obtained as described in the text. A mixture of the polypeptides was directly analyzed with MALDI-TOF mass spectrometry. Other conditions are the same as in the legend to Figure 6.

alkaline condition showed that Tyr218 was indeed the modification site (data not shown). We found that the *O*-carbethoxylation of Tyr218 was only weakly suppressed by the presence of AsA^- in an alkaline condition (Figure 9).

To rule out the possibility of the direct reaction of AsA^- with DEPC (which may lead to the protective effect), we conducted a control experiment using a nonredox protein, insulin (bovine). Bovine insulin consists of A and B chains having two disulfide interchain linkages with a molecular mass of 5733.69 Da (Figure 10, traces **a**, **b**). There are two His, four Tyr, and one Lys residues, in total, as possible DEPC reactive sites. Upon DEPC treatment under a similar condition (in neutral and alkaline pH regions) used for cytochrome b_{561}, we found that there were five reactive sites in intact bovine insulin (Figure 10, trace **c**). Based on the analyses for the separated chains and the tryptic digest (not shown), we tentatively assigned these positions as His5, His10, Tyr15, and Tyr26 in the B chain and either Tyr14 or Tyr19 in the A chain. Among them, the *N*-carbethoxylation of His5 and His10 was most significant. The presence of 20 mM AsA^- during the DEPC treatment did not cause any significant suppression of the carbethoxylation of insulin (Figure 10, trace **d**).

In brief, MALDI-TOF mass analyses showed that the presence of AsA^- during the DEPC treatment protects the heme-coordinating histidyl residues (His88 and His161) from the *N*-carbethoxylation, whereas Lys85 was not rescued from the modification. The *O*-carbethoxylation of Tyr218 was enhanced in an alkaline condition and was partially protected in the presence of AsA^- during the DEPC treatment.

DISCUSSION

The present redox titration experiment clearly shows that purified cytochrome b_{561} contains two heme *b* centers with different midpoint potentials (+60 and +170 mV). DEPC treatment of cytochrome b_{561} in the oxidized state changed its redox behavior. One of the heme *b* centers showed a drastic shift in its midpoint potential from +60 to −30 mV, whereas the other heme center with a higher potential did not show any appreciable influence (Figure 2A,B). This result strongly suggests that *N*-carbethoxylation of the noncoordinating nitrogen atom of imidazole groups in the His−heme *b*−His system causes a lowering of the midpoint potential of the heme *b* with a lower potential, and is fully consistent with our proposal that specific *N*-carbethoxylation of the

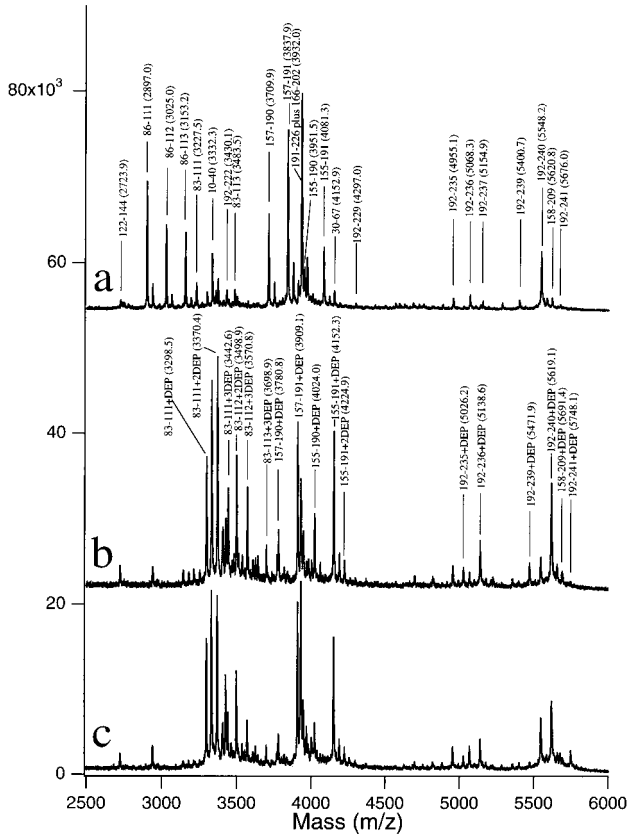

FIGURE 9: MALDI-TOF mass spectra of tryptic digests obtained from the untreated (trace **a**) and the DEPC (0.5 mM)-treated [either in the presence of 20 mM AsA^- (trace **b**) or in the oxidized state (trace **c**)] cytochrome b_{561} in the alkaline condition. Tryptic digests were obtained as described in the text. A mixture of the polypeptides was directly analyzed with MALDI-TOF mass spectrometry. Other conditions are the same as in the legend to Figure 6.

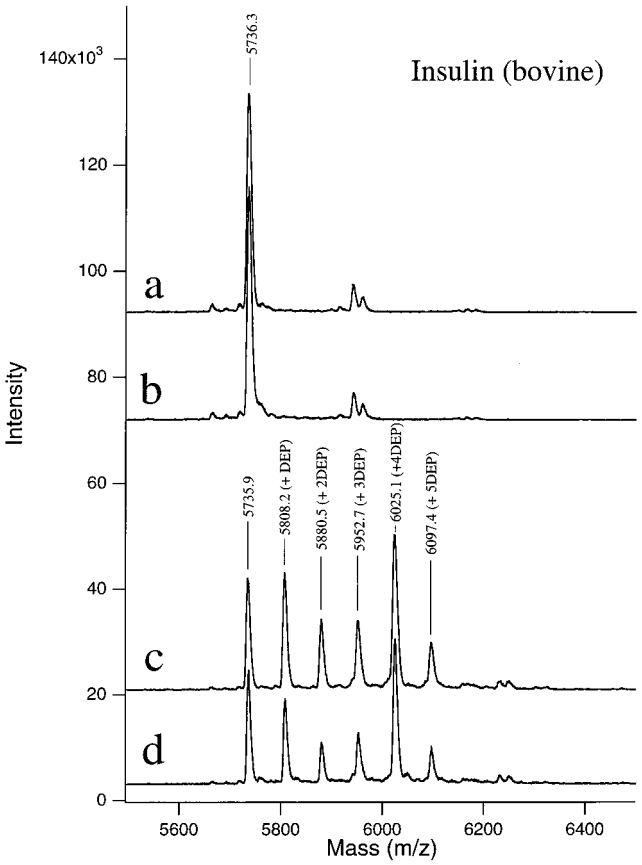

FIGURE 10: Effects of AsA^- on the DEPC modification of bovine insulin. Intact bovine insulin (trace **a**) was treated with 20 mM AsA^- alone (trace **b**) or with 0.5 mM DEPC either in the absence (trace **c**) or in the presence of 20 mM AsA^- (trace **d**) under similar conditions as described in the text and was directly analyzed with MALDI-TOF mass spectrometry.

imidazole ring of the two fully conserved histidyl residues (His88 and His161), which are expected as the heme *b* ligands at the extravesicular side, is responsible for the inhibition of the electron-accepting ability from AsA^- in the medium (*15*). Thus, the final reduction level of heme *b* with AsA^- is dependent on the extent of the modification at the heme-coordinating histidyl residues.

The presence of AsA^- during the DEPC treatment caused a clear protective effect against the shift in midpoint potential, leaving the redox behavior of the sample almost intact (Figure 2B). Such a protective effect of AsA^- against the modification with DEPC was also observed in the 'AsA^--mixing assay' (Figure 3) and the pulse radiolysis study (Figure 4). In each case, the ability of electron acceptance from AsA^- in the medium was almost fully rescued by the inclusion of AsA^- during the DEPC treatment. MALDI-TOF-MS analysis showed that these were indeed the heme-coordinating histidyl residues (His88 and His161) which were protected from the *N*-carbethoxylation upon inclusion of AsA^- (Figures 5−9).

As the cause of the protective effect of AsA^- against DEPC modification, a number of possible mechanisms might be considered. One possible mechanism is that the histidyl residues coordinating to ferrous heme *b* do not react with DEPC. This is supported by the fact that similar protective effects against the DEPC modification were observed for sodium dithionite. Upon reduction of the heme iron with AsA^-, the redistribution of charge at the heme moiety occurs, leading to a spillover of electron equivalents into the coordinating imidazole. This may cause a drastic change in the pK_a of the noncoordinating nitrogen (probably N_δ atom) of the heme-coordinating imidazole ring. It was reported that the reactivity of DEPC is very dependent on the protonation level of imidazole; i.e., only the unprotonated form is reactive (*22*). The pH-dependent inhibition with DEPC of the electron-accepting ability from AsA^- (Figure 3D) seems consistent with this view. For the treatment with DEPC in the oxidized state, the inhibition curve suggests the reactive imidazole to have a pK_a around 5.5, whereas in the reduced state the pK_a seemed to shift to a much higher value, around 7.5 (Figure 3D).

However, the protective effect of AsA^- against the DEPC modification could not be ascribed solely to the redox-dependent shift in pK_a of the histidyl residues. A plausible explanation for the protective effect is the shielding effect by AsA^-. An AsA^- molecule bound at the putative substrate-binding site close to the heme *b* center at the extravesicular side may protect the imidazole group from the access of DEPC. The presence of such an AsA^--binding site on cytochrome b_{561} was proposed based on the study of steady-state electron transfer across chromaffin vesicle membranes (*23, 24*), although the estimated K_m value for AsA^- is very high (~340 μM) (*7*). Since the heme-coordinating histidyl residues (His88 and His161) are expected to locate

very close to the putative AsA^--binding site formed by the fully conserved sequence (^{69}ALLVYRVFR^{77}) (Figure 1) (*14*), it is very likely that they may also participate in substrate binding.

Ascorbic acid exists in protonated, monoanion (AsA^-), and dianion (AsA^{2-}) forms with pK_a values of 4.04 and 11.34 (*24*). The monoanion form (AsA^-), which is predominant at physiological pH, is not a good electron donor for heme *b*. The redox potential of 2 mM AsA^- solution (at pH 6.0) is roughly +300 mV in our potentiometric system (data not shown), consistent with the high midpoint potential value (E_m = +766 mV) of the AsA^-/MDA couple (*24*). At this level of redox potential, there should be no reduction of heme *b* (Figure 2A). Under these conditions, however, the reduction of heme *b* was achieved as high as the 85−90% level (Figure 3A). According to the "concerted proton/electron transfer mechanism" (*23*, *24*), cytochrome b_{561} stabilizes the dianion form of AsA^- at the substrate-binding site by proton transfer to an amino acid residue nearby (or, alternatively, destabilizes the monoanion form by promoting the dissociation of the second proton from bound AsA^-) to utilize the strong reducing power of the dianion form (E_m = +76 mV for the AsA^{2-}/MDA couple). The heme-coordinating histidyl residues, which are likely to have pK_a values around 5.5 in the oxidized state (Figure 3D), may be very suitable for such a proton acceptor from AsA^-.

Lys85 was found as only one major modification site when the DEPC treatment was done in the presence of AsA^- under acidic or neutral pH conditions. Since Lys85 is located at the extravesicular surface of the molecule (Figure 1) and is fully conserved (*14*), it is likely that this positively charged group, in conjunction with other well-conserved positively charged residues, has important roles for the binding/recognition for AsA^-. Cluster of these positive charges at the extravesicular surface may help the AsA^- molecule to approach the AsA^--binding site formed by the fully conserved sequence (^{69}ALLVYRVFR^{77}) (*14*) and the heme-coordinating histidyl residues (His88 and His161). The apparent absence of the protective effect of AsA^- against the modification of Lys85, however, suggests that the binding of the AsA^- molecule to this region is not tight enough to shield it from the access of DEPC.

Tyr218 may have a very important role for the recognition and/or binding of AsA^- as well. DEPC treatment of oxidized cytochrome b_{561} in an alkaline condition caused a specific and significant *O*-carbethoxylation of this residue, in addition to the *N*-carbethoxylation of Lys85, His88, and His161. Concomitantly, the fast electron transfer from AsA^- to oxidized heme *b* became even slower, compared to the DEPC-treated sample in the neutral pH region. We observed further that AsA^- had a clear protective effect against the DEPC modification of Tyr218. These observations are consistent with our suggestion that this residue is also a part of the putative binding/recognition site for AsA^-. Indeed this residue is well conserved among various species and is located at the extravesicular side of the molecule (*14*). It must be noted that the DEPC modifications of Lys85 and Tyr218 affected only the rate of the fast electron transfer process from AsA^- and did not affect significantly the final reduction level of heme *b*.

We observed that the second phase after pulse radiolysis (i.e., heme *b* reduction phase) was fully protected from DEPC inactivation in the presence of 20 mM AsA^- (Figure 4). However, this observation is, at first glance, inconsistent with the results obtained for the 'AsA^--mixing assay' using oxidized cytochrome b_{561} and AsA^- (Figure 3B). The latter indicated that oxidized cytochrome b_{561} pretreated with DEPC in the presence of 20 mM AsA^- has a slower reaction process with AsA^- compared to the control sample. (This might be attributed to the *N*-carbethoxylation of Lys85, which could not be protected by the presence of AsA^- during the DEPC modification.) Although we ascribed previously that the second phase after pulse radiolysis was due to the bimolecular reaction of AsA^- with oxidized cytochrome b_{561} (*13*), it is actually a mixture of two processes: the intramolecular electron transfer from the extravesicular heme *b* to the intravesicular heme *b* and the rereduction of the extravesicular heme *b* with AsA^-. When the DEPC treatment was done in the oxidized state, the heme *b* center at the extravesicular side could not accommodate an electron equivalent from AsA^- due to a drastic change in the midpoint potential. Thus, neither the intramolecular electron transfer reaction nor the reduction with AsA^- occurred after pulse radiolysis. If the DEPC treatment was conducted in the presence of 20 mM AsA^-, both hemes *b* could accommodate electron equivalents from AsA^- after a longer incubation and, therefore, the intramolecular electron transfer could take place after the pulse radiolysis.

It is very important to note that *N*-carbethoxylation of amino acid residues occurs selectively in the extravesicular side. There are three histidyl residues in addition to lysyl (four) and tyrosyl (six) residues in the intravesicular side. Except for Tyr192 (*15*), none of these residues showed the reactivity toward DEPC. In the present study, all the experimental treatments were conducted in the presence of 1.0% (w/v) octyl β-glucoside, at a much higher concentration than the CMC value of octyl β-glucoside (23 mM). Thus, cytochrome b_{561} is considered to exist in a monomeric form surrounded by detergent molecules for the part of hydrophobic membrane-spanning helices. The extravesicular and intravesicular sides are likely to be exposed to the medium. Since a water-soluble MDA radical can receive an electron equivalent very efficiently from the reduced heme *b* at the intravesicular side, the possibility that cytochrome b_{561} exists as an oligomeric state to obstruct the access of DEPC to the intravesicular side can be ruled out. Probably, the conformation of the intravesicular side may be so unusual that DEPC cannot approach those residues.

Present results, in conjunction with our previous studies, provide a clearer view for the trans-membrane electron transfer catalyzed by cytochrome b_{561} specific to the neuroendocrine vesicles. In the oxidized state, two histidyl ligands (His88 and His161) of the heme *b* center at the extravesicular side and one tyrosyl residue (Tyr218) and one lysyl (Lys85) residue could be selectively carbethoxylated with DEPC. These modifications lead to the selective loss of the electron acceptance from AsA^- by a drastic decrease of the midpoint potential of heme *b* at the extravesicular side. Both the carbethoxylation of His88, His161, and Tyr218 and the loss of the electron-accepting ability were inhibited by the inclusion of AsA^- during the DEPC treatment. The protective effect of AsA^- was explained as being due to a shift of the pK_a of the imidazole group in the reduced state and the shielding effect of AsA^- against the access of DEPC

to the AsA^--binding site. The presence of the two histidyl ligands (His88 and His161) at the AsA^--binding site suggests that they may have an additional role as a proton acceptor from AsA^- to utilize the reducing power of its dianion form. Tyr218, together with Lys85, has a role in the recognition/binding process for AsA^- and is indispensable for the fast electron transfer reaction from AsA^-. Further studies are in progress to reveal the detailed intramolecular electron transfer reaction.

ACKNOWLEDGMENT

We thank the members of the Radiation Laboratory at the Institute of Scientific and Industrial Research, Osaka University, for assistance in operating the accelerator.

REFERENCES

1. Eipper, B. A., Mains, R. E., and Glembotski, C. C. (1983) *Proc. Natl. Acad. Sci. U.S.A. 80*, 5144−5148.
2. Kent, U. M., and Fleming, P. J. (1987) *J. Biol. Chem. 262*, 8174−8178.
3. Dhariwal, K. R., Black, C. D. V., and Lavine, M. (1991) *J. Biol. Chem. 266*, 12908−12914.
4. Njus, D., Knoth, J., Cook, C., and Kelley, P. M. (1983) *J. Biol. Chem. 258*, 27−30.
5. Njus, D., Kelley, P. M., and Harnadek, G. J. (1986) *Biochim. Biophys. Acta 853*, 237−265.
6. Wakefield, L. M., Cass, A. E. G., and Radda, G. K. (1986) *J. Biol. Chem. 261*, 9739−9745.
7. Flatmark, T., and Terland, O. (1971) *Biochim. Biophys. Acta 253*, 487−491.
8. Duong, L. T., Fleming, P. J., and Russell, J. T. (1984) *J. Biol. Chem. 259*, 4885−4889.
9. Pruss, R. M., and Shepard, E. A. (1987) *Neuroscience 22*, 149−157.
10. Silsand, T., and Flatmark, T. (1974) *Biochim. Biophys. Acta 359*, 257−266.
11. Duong, L. T., and Fleming, P. J. (1982) *J. Biol. Chem. 257*, 8561−8564.
12. Tsubaki, M., Nakayama, M., Okuyama, E., Ichikawa, Y., and Hori, H. (1997) *J. Biol. Chem. 272*, 23206−23210.
13. Kobayashi, K., Tsubaki, M., and Tagawa, S. (1998) *J. Biol. Chem. 273*, 16038−16042.
14. Okuyama, E., Yamamoto, R., Ichikawa, Y., and Tsubaki, M. (1998) *Biochim. Biophys. Acta 1383*, 269−278.
15. Tsubaki, M., Kobayashi, K., Ichise, T., Takeuchi, F., and Tagawa, S. (2000) *Biochemistry 39*, 3276−3284.
16. Dutton, P. L. (1978) *Methods Enzymol. 54*, 411−435.
17. Kobayashi, K., Harada, Y., and Hayashi, K. (1991) *Biochemistry 30*, 8310−8315.
18. Kobayashi, K., Tagawa, S., Sano, S., and Asada, K. (1995) *J. Biol. Chem. 270*, 27551−27554.
19. Perin, M. S., Fried, V. A., Slaughter, C. A., and Südhof, T. C. (1988) *EMBO J. 7*, 2697−2703.
20. Apps, D. K., Boisclair, M. D., Gavine, F. S., and Pettigrew, G. W. (1984) *Biochim. Biophys. Acta 764*, 8−16.
21. Kamensky, Y. A., Arutjunjan, A. M., Konstantinov, A. A., Moroz, I. A., and Burbaev, D. S. (1989) in *International Symposium "Molecular Organization of Biological Structures"*, pp A2−7, Moscow.
22. Miles, E. W. (1977) *Methods Enzymol. 47*, 431−442.
23. Jalukar, V., Kelley, P. M., and Njus, D. (1991) *J. Biol. Chem. 266*, 6878−6882.
24. Njus, D., and Kelley, P. M. (1993) *Biochim. Biophys. Acta 1144*, 235−248.

BI002240X